Modern Valence-Bond Description of Homoaromaticity

Peter B. Karadakov*,† and David L. Cooper*,‡

†*Department of Chemistry, University of York, Heslington, York, YO10 5DD, U.K.*

‡*Department of Chemistry, University of Liverpool, Liverpool L69 7ZD, U.K.*

Abstract

Spin-coupled (SC) theory is used to obtain modern valence-bond (VB) descriptions of the electronic structures of local minimum and transition state geometries of three species that have been considered to exhibit homoconjugation and homoaromaticity: the homotropenylium ion, $C_8H_9^+$, the cycloheptatriene neutral ring, C_7H_8, and the 1,3-bishomotropenylium ion, $C_9H_{11}^+$. The resulting compact SC wavefunctions are of comparable quality to CASSCF constructions that are based on the same "N electrons in M orbitals" active spaces, but they are much easier to interpret directly. Analysis of the forms of the SC orbitals and of the overlaps between them, as well as an examination of the compositions of the associated resonance patterns, strongly suggest that both of the homotropenylium and 1,3-bishomotropenylium ions are homoaromatic at their local minimum geometries, with all of the other cases that were considered being non-aromatic. The SC results also show that the differences between "no-bond" and "bond" homoconjugated systems are very likely to be much smaller than previously thought.

1 Introduction

Homoconjugation and homoaromaticity (a detailed account of the history of these concepts can be found in refs 1–3) are usually interpreted using a simple orbital model: In a homoconjugated system, the continuous chain of p_π orbitals contributed by sp^2 hybridized atoms is interrupted by one or more non-neighboring sp^3 hybridized atoms but the p_π orbital overlaps involving centers connected to a sp^3 hybridized atom remain sufficiently large so as to sustain conjugation; a homoaromatic molecule, following the well-known Hückel rule, includes a homoconjugated cycle with $4n + 2$ π electrons. A classical example of a Hückel-type homoaromatic molecule is provided by the homotropenylium ion, $C_8H_9^+$ (often referred to as homotropylium). This ion features an eight-membered ring involving seven sp^2 hybridized carbons, ordered very much as in the tropylium ion, $C_7H_7^+$, but with the addition of a methylene bridge jutting out of the nearly planar seven-atom arrangement. It is also possible to define and to explore Möbius-type homoaromaticity, utilizing a $4n$ electrons rule.[4]

Support for this simple orbital model of homoconjugation is usually sought through visual examination of the delocalization patterns of the molecular orbitals (MOs) from Hartree-Fock (HF) or Kohn-Sham density functional theory (DFT) calculations. However, analyses of this type do not provide details about the extent to which an intervening sp^3 hybridized atom changes the sequence of p_π orbital overlaps in the homoconjugated chain. It is also important to remember that examination of individual MO shapes becomes less relevant in post-HF approaches which make use of multiconfiguration wavefunctions that correspond to MOs with fractional occupation numbers.

On the other hand, valuable insights into the electronic structure of homoaromatic molecules can be gained by analyzing the total electron density through Bader's Atoms in Molecules (AIM) approach,[5] or through the related topological analysis of the electron localization function (ELF).[6] Early work[7] found a bond critical point along the path linking the carbon atoms that are connected to the intervening methylene group in the homotropenylium ion. This was taken to indicate homoconjugation and bond homoaromaticity in this system. However, a detailed AIM analysis of the total electron density in the homotropenylium ion at more reliable geometries[1] showed that it should be viewed as a "no-bond" homoaromatic system; this is also supported by the ELF results of Lepetit *et al.*[8] Interestingly, these ELF results suggest that the weights of the "resonance forms" for the homotropenylium ion, in which the p_π orbitals on both sides of the methylene group form a bond, are equal to zero, while the other "resonance forms" are of equal weight. Cremer *et al.* have formulated a set of AIM-based rules for "bond" homoaromaticity and "no-bond" homoaromaticity;[1] an alternative set of ELF-based rules has been defined by Lepetit *et al.*[8]

In this paper we use spin-coupled (SC) theory to obtain modern valence bond (VB) descriptions of the electronic structures of certain potentially homoaromatic species: the homotropenylium ion, $C_8H_9^+$, the cycloheptatriene neutral ring, C_7H_8, the homoaromaticity of which was established by Schleyer *et al.*,[2] and the 1,3-bishomotropenylium ion, $C_9H_{11}^+$, which features two sp^3 hybridized carbons.[9]

In its original form,[10,11] the SC wavefunction is equivalent to the full generalized valence bond (full-GVB) wavefunction[12] and includes a "N electrons in N orbitals" active space, in which a single product of N non-orthogonal active orbitals is multiplied by a general N-electron spin function. In most applications, the SC(N, N) [or simply, SC(N)] wavefunction provides a close approximation to the corresponding "N in N" complete-active-space self-consistent field (CASSCF) wavefunction. The SC(N) wavefunction typically proves much easier to interpret, not least because it can be represented in terms of a relatively small number of VB resonance structures, the most important of which are usually found to be the ones expected from chemical intuition (for a review, see ref 13). An easy-to-follow example is provided by the SC description of the π-electron system of benzene.[14–16] The six π electrons are placed in a single product of six non-orthogonal active (or SC) orbitals, the spins of which are coupled in all five possible ways that lead to an overall singlet. The optimal SC orbitals turn out to be well-localized, similar in shape to C($2p_\pi$) atomic orbitals with small symmetrical protrusions towards neighboring carbons, while the optimal spin-coupling pattern, if expressed in terms of Rumer spin functions,[17] reveals the presence of two equivalent dominant Kekulé-like structures and three less important equivalent Dewar-like (or para-bonded) structures. This SC picture reproduces the essential features of the well-known classical VB description of benzene in terms of resonance structures, and comes from a wavefunction which accounts for almost 90% of the "non-dynamic" correlation energy incorporated in a "6 in 6" π-space CASSCF [CASSCF(6,6)] wavefunction.[16] An extension of SC theory to "N in M" ($N \neq M$) active spaces was introduced in ref 18. The SC(N, M) wavefunction retains the essential features of the original SC model: It includes just the products of non-orthogonal orbitals corresponding to all distributions of N electrons amongst M orbitals in which the smallest number of orbitals possible, $|N - M|$, are doubly-occupied (for $N > M$) or omitted (for $N < M$), and all other orbitals are singly-occupied; each of these products is combined with a flexible spin function which permits any allowed mode of coupling of the spins of the orbitals within the product.

We show here that SC theory is capable of producing convincing highly visual orbital models of the electronic structures of homoaromatic molecules that can provide direct numerical estimates of quan-

tities that are difficult to access through alternative approaches. Such quantities include the overlaps between consecutive active orbitals around the ring, including those associated with atoms connected to a sp^3 hybridized carbon, and the extents to which different spin-coupling patterns (that can be linked to VB resonance structures) contribute to the overall wavefunction.

2 Results and Discussion

The gas-phase ground state geometries of the homotropenylium ion, neutral cycloheptatriene and the 1,3-bishomotropenylium ion were optimized using second-order Møller-Plesset perturbation theory with the cc-pVTZ basis, including all orbitals in the correlation treatment [MP2(Full)/cc-pVTZ]. For each of these systems we obtained a local minimum geometry of C_s symmetry and a transition state (TS) geometry of C_{2v} symmetry (see Figure 1). In the case of the 1,3-bishomotropenylium ion we could also locate two additional tricyclic local minima, of C_s and C_2 symmetry, corresponding to *cis* and *trans* arrangements of the methylene groups, respectively (see Figure 2). As the best known theoretical geometry of the homotropenylium ion is the MP2(Full)/6-31G(d) one reported by Cremer *et. al.*,[19] we carried out additional optimizations of the respective local minimum and TS geometries of the homotropenylium ion at this level of theory (see Figure 1); our MP2(Full)/6-31G(d) local minimum and TS geometries are identical to those from ref 19. The local minimum or TS character of each optimized geometry was verified through a calculation of analytical harmonic vibrational frequencies. All of these calculations were performed with GAUSSIAN09,[20] using the "VeryTight" convergence criteria in geometry optimizations.

Place Figure 1 near here.
Place Figure 2 near here.

The vibrational frequencies of the C_s symmetry local minimum geometries of the homotropenylium ion calculated at the MP2(Full)/cc-pVTZ and MP2(Full)/6-31G(d) levels are reasonably similar (the lowest four of these are given in Table 1). However, an analogous comparison for the C_{2v} symmetry TS geometries reveals pronounced decreases in $i\tilde{\nu}_1$, $\tilde{\nu}_2$ and $\tilde{\nu}_3$ at the MP2(Full)/6-31G(d) level. This suggests that the MP2(Full)/6-31G(d) TS geometry might be affected by the so-called "insidious two-electron intramolecular basis set incompleteness error", due to which popular quantum chemical methods, including MP2, in combination with certain basis sets, may erroneously predict that benzene and certain arenes are nonplanar[21] (see also ref 22). As a result of this observation, we consider the MP2(Full)/cc-pVTZ geometries to be more reliable than those from MP2(Full)/6-31G(d). It should be noted that the MP2(Full)/cc-pVTZ C_s symmetry local minimum geometry of the homotropenylium ion shows a slightly lower extent of carbon-carbon bond equalization in comparison to its MP2(Full)/6-31G(d) counterpart (see Figure 1). Our MP2(Full)/cc-pVTZ local minimum geometry for cycloheptatriene is very similar to the MP2/def2-TZVP geometry reported by Sundholm *et al.*[23]

Place Table 1 near here.

Given that we are using SC theory, an active space approach, to describe the electronic structures of popular examples of potentially homoaromatic species, we need to specify the sizes of the active spaces appropriate for the homotropenylium ion (**1**, **1**-TS), neutral cycloheptatriene (**2**, **2**-TS) and the 1,3-bishomotropenylium ion (**3**, **3**-TS) (see Figure 1). Clearly, each of **1**, **1**-TS, **3** and **3**-TS requires a "6 in 7" active space, whereas **2** and **2**-TS require "6 in 6" active spaces. However, the tricyclic **3**-*cis* and **3**-*trans* (see Figure 2) would require larger active spaces, at least "10 in 11", if we were to include in the active space the orbitals describing two bonds from each cyclopropyl ring (those above and/or below the seven-membered ring); the required active space size would of course increase even further if, for consistency, it was extended so as to include orbitals that describe the additional predominantly σ bonds.

Considerations along these lines suggest that active space methods, such as SC and CASSCF, are not the most appropriate for systems exhibiting "bond" homo(anti)aromaticity following from cyclopropyl homoconjugation.[1] As a consequence, we focus in this paper on the "no-bond" potentially homoaromatic systems **1**, **2** and **3** and on the corresponding transition states **1**-TS, **2**-TS and **3**-TS.

We carried out fully-variational SC(6,7) and CASSCF(6,7) calculations for **1**, **1**-TS, **3** and **3**-TS, and fully-variational SC(6) and CASSCF(6,6) calculations for **2** and **2**-TS. We used the cc-pVTZ basis in all of these calculations and the geometries that we optimized at the MP2(Full)/cc-pVTZ level of theory. All SC calculations were performed by means of the CASVB algorithms[24–27] implemented in MOLPRO;[28,29] all CASSCF results were obtained with both GAUSSIAN09[20] and MOLPRO.[28,29]

The SC(6,7) wavefunction used for **1**, **1**-TS, **3** and **3**-TS can be written in the following form:

$$\begin{aligned}\Psi_{00}(6,7) = \hat{\mathcal{A}}\big[(\text{core})\big(&\psi_2\psi_3\psi_4\psi_5\psi_6\psi_7\Theta^6_{1;00} \\ &+ \psi_3\psi_4\psi_5\psi_6\psi_7\psi_1\Theta^6_{2;00} + \psi_4\psi_5\psi_6\psi_7\psi_1\psi_2\Theta^6_{3;00} + \psi_5\psi_6\psi_7\psi_1\psi_2\psi_3\Theta^6_{4;00} \\ &+ \psi_6\psi_7\psi_1\psi_2\psi_3\psi_4\Theta^6_{5;00} + \psi_7\psi_1\psi_2\psi_3\psi_4\psi_5\Theta^6_{6;00} + \psi_1\psi_2\psi_3\psi_4\psi_5\psi_6\Theta^6_{7;00}\big)\big]\end{aligned} \tag{1}$$

where "(core)" denotes the doubly-occupied orbitals accommodating the core electrons (25 core orbitals for **1** and **1**-TS, and 29 core orbitals for **3** and **3**-TS), and the ψ_μ are singly-occupied nonorthogonal SC (or active) orbitals. The "00" subscripts indicate the values of the total spin S and its z-projection, *i.e.* M_S, $S = M_S = 0$. In this expression, $\Theta^6_{\nu;00}$ denotes a general $S = M_S = 0$ six-electron spin function associated with the SC orbital product that omits SC orbital ψ_ν,

$$\Theta^6_{\nu;00} = \sum_{k=1}^{5} C_{\nu;0k}\Theta^6_{00;k} \tag{2}$$

where $\Theta^6_{00;1}$–$\Theta^6_{00;5}$ stand for the five linearly independent six-electron singlet spin functions expressed in a suitable spin basis. Note that the $\Theta^6_{\nu;00}$ functions are not individually normalized, so that the variationally-determined $C_{\nu;0k}$ coefficients take into account the relative importance of the orbital product labelled ν in the final wavefunction. **2** and **2**-TS were described using a more compact traditional SC(6) wavefunction with 22 doubly-occupied core orbitals,

$$\Psi_{00}(6) = \hat{\mathcal{A}}\big[(\text{core})\psi_1\psi_2\psi_3\psi_4\psi_5\psi_6\Theta^6_{00}\big] \tag{3}$$

in which Θ^6_{00} is defined analogously to the spin function in Eq. (2), but dropping the (now superfluous) orbital product index ν.

As usual, the core and SC orbitals were approximated, just as in molecular orbital (MO) theory, by linear expansions in the full cc-pVTZ basis set for the respective molecule. All of the orbital coefficients and spin-coupling coefficients, $C_{\nu,0k}$ or C_{0k}, were determined variationally, by minimizing the energy expectation value of the SC wavefunction. In order to obtain clearer VB-style descriptions for **1**-TS and **3**, two additional SC(6,7) calculations were carried out maintaining, in each case, orthogonality between a pair of SC orbitals (*vide infra*). These constraints turned out to have very low impacts on the converged SC energies, amounting to under 0.3 mE_h for **1**-TS and under 0.2 mE_h for **3**, but led to much easier to interpret solutions.

The total energies of the HF, SC and CASSCF wavefunctions for the "no-bond" homoaromatic systems **1**, **2** and **3**, and the corresponding transition states **1**-TS, **2**-TS and **3**-TS, and the percentages of CASSCF correlation energy accounted for by the SC wavefunctions are shown in Table 2, together with

Place Table 2 near here.

the numbers of configuration state functions (CSFs) included in each SC or CASSCF wavefunction. The percentages of CASSCF correlation energy recovered by the SC wavefunctions for all homoaromatic systems studied in this paper are very high, well above the 89.5% achieved by the SC(6) wavefunction for benzene [measured against CASSCF(6,6), cc-pVTZ basis[18]]. This is an indication that the respective SC wavefunctions provide very close approximations to the corresponding CASSCF constructions despite making use of much smaller numbers of CSFs.

The symmetry-unique SC orbitals from the SC(6,7) wavefunctions for **1** and **1**-TS are shown in Figure 3. With the exception of ψ_7 in **1** (and its symmetry-related partner ψ_1), the SC orbitals look like C($2p_\pi$) atomic orbitals with small protrusions towards one or both neighboring carbons. Orbital ψ_4, in both **1** and **1**-TS, closely resembles a SC orbital in benzene (for a picture in a similar style, see ref 18). Orbitals ψ_7 and its symmetry-related partner ψ_1 in **1** extend over two centers each which allows these orbitals to overlap more efficiently across the methylene bridge. The shape of ψ_7 suggests that, in addition to the C($2p_\pi$) character which is spread unevenly between the carbons on the two sides of the methylene bridge, this orbital has some C(2s) character; as a result, the bonding interaction between ψ_7 and ψ_1 across the methylene bridge has elements of both σ and π bonds.

Place Figure 3 near here.

The existence of a well-defined bonding interaction between ψ_7 and ψ_1 shows that the differences between "no-bond" and "bond" homoconjugated systems are much smaller than previously thought; it is not difficult to imagine how the shapes of ψ_7 and ψ_1 would evolve into typical sp^3 hybrids as the distance was reduced between the two carbon atoms on either side of the methylene bridge. On the other hand, increasing the distance between these carbons, as in **1**-TS, makes these two orbitals much more C($2p_\pi$)-like. The rather different shape of ψ_7 in **1**-TS, and its wider separation from the corresponding ψ_1, strongly suggest that the interaction between these two orbitals should be rather weak. An example intermediate between **1** and **1**-TS can be seen in a SC study of bicyclic 1,6-methano[10]annulene ("homonaphthalene")[30] which describes an interaction between SC orbitals across a methylene bridge over a distance of 2.125 Å. The SC orbitals reported in ref 30 still have some two-center character but are much more C($2p_\pi$)-like than those in **1**.

These observations are reinforced by the overlap integrals between the SC orbitals in **1** and in **1**-TS, listed in Table 3. The $\langle\psi_1|\psi_7\rangle$ overlap of 0.498 in **1** is the largest overlap between adjacent SC orbitals for this structure, whereas the corresponding overlap in **1**-TS is very low, just 0.005. The overlap integrals between adjacent SC orbitals in **1**, taken in the sequence $\langle\psi_1|\psi_2\rangle$, $\langle\psi_2|\psi_3\rangle$, $\langle\psi_3|\psi_4\rangle$, $\langle\psi_4|\psi_5\rangle$, $\langle\psi_5|\psi_6\rangle$, $\langle\psi_6|\psi_7\rangle$, $\langle\psi_1|\psi_7\rangle$, show a fair degree of equalization; the overlap integrals from this sequence are comparable to the overlap integrals of 0.435 for adjacent SC orbitals in the tropylium cation.[18] We observe lower values (0.358) for the identical overlaps $\langle\psi_1|\psi_2\rangle = \langle\psi_6|\psi_7\rangle$. The overlap integrals from the analogous sequence in **1**-TS exhibit pronounced alternation: the values of $\langle\psi_1|\psi_2\rangle = \langle\psi_6|\psi_7\rangle$ and $\langle\psi_2|\psi_3\rangle = \langle\psi_5|\psi_6\rangle$ are consistent with the π components of "double" and "single" carbon-carbon bonds, respectively, in a conjugated system, whereas $\langle\psi_3|\psi_4\rangle = \langle\psi_4|\psi_5\rangle$ are very close to the overlap integrals of 0.525 between adjacent SC orbitals in benzene.[18] Due to the shorter distances between non-adjacent carbon atoms in **1**, the overlap integrals between SC orbitals based on such atoms are larger in magnitude than their counterparts in **1**-TS; however, none of the overlap integrals between non-adjacent SC orbitals in **1** and **1**-TS are large enough to suggest important bonding interactions.

Place Table 3 near here.

The pair of SC orbitals constrained to be orthogonal in the SC(6,7) calculation for **1**-TS were ψ_3 and ψ_5. The data in Table 3 shows that this constraint should have only a very minor effect on the active space orbitals, given that it sets to zero a small overlap between non-adjacent SC orbitals; the magnitude

of the corresponding $\langle\psi_3|\psi_5\rangle$ overlap in **1** is just 0.066.

The relative importance of the different six-electron singlet spin functions participating in the SC(6,7) wavefunctions for **1** and for **1**-TS are illustrated in Figure 4, which shows all spin functions with Chirgwin-Coulson weights[31] higher than 3%. It proved most informative in the present study to work in the Rumer spin basis.[17] All of the Chirgwin-Coulson weights are calculated within the spin space which, for the SC(6,7) wavefunction from Eq. (1), is given by $\Theta^6_{1;00} + \Theta^6_{2;00} + \ldots + \Theta^6_{7;00}$ and, for the SC(6) wavefunction from Eq. (3), by Θ^6_{00}. The Rumer spin functions shown in Figure 4 are represented through appropriately modified Rumer diagrams, which allow a direct link to the concept of resonance used in classical VB theory. The numbers 1–7 in each diagram correspond to SC orbitals ψ_1–ψ_7 and the σ bond framework is shown by lines connecting these numbers, whereas singlet two-electron active space spin functions are denoted either as "double" bonds, or using dotted lines for orbitals on centers that are not connected by σ bonds. For example, the third diagram in the top row of Figure 4 corresponds to the Rumer spin function

Place Figure 4 near here.

$$(1-7, 2-3, 4-5) = 2^{-3/2}[\alpha(1)\beta(7) - \alpha(7)\beta(1)][\alpha(2)\beta(3) - \alpha(3)\beta(2)][\alpha(4)\beta(5) - \alpha(5)\beta(4)] \quad (4)$$

The seven most important Rumer spin functions in **1**, with a combined weight of *ca.* 54%, are all Kekulé-style and equivalent to those participating in the seven most important symmetry-equivalent VB structures in the tropylium cation.[18] Each of these Rumer spin functions couples to singlets the spins of three pairs of neighboring SC orbitals, creating either three almost π bonds as, for example, in $(1-2, 3-4, 5-6)$, or two almost π bonds and a bond across the methylene bridge as, for example, in $(1-7, 2-3, 4-5)$. Closer examination reveals that all of the Rumer spin functions from the top row of Figure 4 involve a hexatriene-like conjugated fragment composed of either a sequence of three almost π bonds, or a sequence of two almost π bonds and a bond across the methylene bridge. Having the bond across the methylene bridge at the end of the hexatriene-like conjugated fragment, as in $(1-7, 2-3, 4-5)$ and $(1-7, 3-4, 5-6)$, turns out to be only slightly less favorable than having a hexatriene-like conjugated fragment that features three almost π bonds, as in $(1-2, 3-4, 5-6)$ and $(2-3, 4-5, 6-7)$. Having the bond across the methylene bridge in the middle of the hexatriene-like conjugated fragment, as in $(1-7, 2-3, 5-6)$, turns out to be less efficient, but this is still more advantageous than the situation in $(1-2, 3-4, 6-7)$ and $(1-2, 4-5, 6-7)$, where the bond across the methylene bridge turns out to be less capable of sustaining conjugation than is a carbon-carbon single bond, and so we end up with combinations of butadiene-like and ethene-like conjugated fragments. All of the remaining Rumer spin functions in **1** with individual weights higher than 3% involve one "long diagonal" bond; VB structures including Rumer spin functions of this type were also found to be the second most important ones in the tropylium cation.[18] Taken together, the Rumer spin functions for **1** shown in Figure 4 account for a considerable part, a little over 84%, of the spin space. The shapes of the SC orbitals for **1**, the overlaps between them and the composition of the spin space all strongly suggest that the electronic structure of **1** closely resembles that of the tropylium cation,[18] and that **1** is aromatic, but less so than the tropylium cation.

It is interesting to compare the SC picture of the resonance in **1** to the ELF results of Lepetit *et al.*[8] According to the ELF analysis, which considers "resonance forms" corresponding only to the Kekulé-style Rumer spin functions, the combined weight of the "resonance forms" corresponding to the first two Rumer spin functions for **1** from Figure 4, and the combined weight of the "resonance forms" corresponding to the Rumer spin functions in positions 6 and 7, are identical and equal to 50%, whereas

the weights of the "resonance forms" involving a 1–7 "bond" (corresponding to the Rumer spin functions in positions 3, 4, and 5) are all equal to zero. SC theory agrees with ELF on the importance of the first two Rumer spin functions in Figure 4 but, due to the existence of a well-defined bonding interaction between ψ_1 and ψ_7, assigns (through the variational optimization of the wavefunction) rather different weights to all of the other Kekulé-style Rumer spin functions.

The increased distance in **1**-TS between the carbon atoms on either side of the methylene bridge not only changes the shapes of SC orbitals ψ_1 and ψ_7, and decreases the overlap between them, but it also leads to a very different composition for the spin space, relative to that for **1** (see Figure 4). None of the spin functions for **1**-TS with individual weights higher than 3% feature singlet coupling between ψ_1 and ψ_7; indeed, the combined weight of all spin functions for **1**-TS that include this type of singlet coupling is just 1.4%, as opposed to 38.0% in **1**. This result, taken together with the observations made previously about the shapes of the SC orbitals for **1**-TS and the overlaps between them, indicates that the electronic structure of **1**-TS resembles that of a non-aromatic open-chain heptatrienyl cation. The most important Rumer spin functions in **1**-TS, the symmetry-equivalent $(1-2, 3-4, 6-7)$ and $(1-2, 4-5, 6-7)$, with a weight of 34.8% each (*cf.* the much lower weights of the corresponding spin functions in **1**, just 4.3% each) account for the resonance associated with the possibility of placing the positive charge at positions 5 or 3, respectively. This type of resonance would also be observed in an allyl cation described using a SC(2,3) wavefunction, the SC orbitals in which would be very similar to ψ_3, ψ_4 and ψ_5. We find no evidence to suggest that **1**-TS might be antiaromatic, as was argued in Refs. 32,33; it seems unlikely that using a SC(10,11) wavefunction to include in the active space also the two aliphatic C–H bonds from the methylene group space would result in a resonance pattern that could be identified as antiaromatic.

We turn now to the results for the cycloheptatriene neutral ring, C_7H_8. The symmetry-unique SC orbitals from the SC(6) wavefunctions for **2** and for **2**-TS are shown in Figure 5, the overlaps between the SC orbitals for these systems are listed in Table 4, and the Chirgwin-Coulson weights of the Rumer spin functions from the corresponding spin spaces are reported in Figure 6 (the Rumer diagrams included in this figure follow the conventions adopted in Figure 4). In contrast to the situation observed for **1** and **1**-TS, the differences between SC orbital shapes, overlaps and spin space compositions for **2** and **2**-TS are considerably smaller. This can be attributed to the large separations between the carbon atoms on the two sides of the methylene bridge in each of these structures, 2.354 Å in **2** and 2.587 Å in **2**-TS (see Figure 1). The overlap integral $\langle\psi_1|\psi_6\rangle$ and the weights of the Rumer spin functions that feature singlet coupling between ψ_1 and ψ_6, $(1-6, 2-3, 4-5)$ and $(1-6, 2-5, 3-4)$, are all slightly larger in **2** than in **2**-TS, suggesting a weak bonding interaction across the methylene bridge which is, however, insufficient to allow the establishment of overlap and resonance patterns that are similar to those in benzene. The various features of the SC(6) wavefunctions for **2** and **2**-TS that are displayed in Figures 5 and 6 and in Table 4 indicate that the electronic structures of both of these systems resemble that of 1,3,5-hexatriene. This finding implies that both of **2** and **2**-TS are non-aromatic whereas, according to Sundholm *et al.*,[23,34] the ring-current strength in **2**, calculated using the gauge-including magnetically induced current method (GIMIC),[34] is about half the benzene value, suggesting that **2** is half as aromatic as benzene. The SC results reported here show instead that the differences between the aromaticities of **2** and benzene are much more substantial.

Place Figure 5, Table 4 and Figure 6 near here.

Whereas **2** and **2**-TS featured relatively large distances between the carbon atoms on either side of the methylene bridge, the results of our MP2(Full)/cc-pVTZ geometry optimizations show that the corresponding distances for both of the methylene bridges in **3** are slightly shorter than in **1** (see Figure 1).

This suggests that it would be reasonable to expect some common features in the SC(6,7) descriptions of **1** and **3**. The symmetry-unique SC orbitals from the SC(6,7) wavefunctions for **3** and for **3**-TS are shown in Figure 7. Clearly, ψ_3 in **3** is very similar in shape to ψ_4 in **1**, and ψ_4 in **3** is similar in shape to both ψ_5 and ψ_6 in **1**. The next two SC orbitals in **3**, ψ_5 and ψ_6, overlap across one of the methylene bridges and closely resemble their counterparts in **1**, orbitals ψ_7 and ψ_1. However, a comparison of the overlap integrals between adjacent SC orbitals in **1** and in **3** reveals some significant differences (see Tables 3 and 5 and Figure 8). The orbital overlaps across the slightly shorter methylene bridges in **3**, $\langle\psi_5|\psi_6\rangle = \langle\psi_1|\psi_7\rangle$, are somewhat larger than the corresponding overlap in **1**, $\langle\psi_1|\psi_7\rangle$, suggesting stronger bonding interactions. The overlaps $\langle\psi_2|\psi_3\rangle = \langle\psi_3|\psi_4\rangle$ in **3** are also larger than their counterparts in **1**, $\langle\psi_3|\psi_4\rangle = \langle\psi_4|\psi_5\rangle$. All of the other overlaps between adjacent SC orbitals in **3** are considerably lower, especially the overlap $\langle\psi_6|\psi_7\rangle$ between neighboring orbitals engaged in bonds across different methylene bridges. Overall, the alternation in the values of the overlaps between adjacent SC orbitals around the ring in **3** is significantly more pronounced than in **1** (see Figure 8). The overlaps between SC orbitals across a methylene bridge in **3**-TS, $\langle\psi_5|\psi_6\rangle = \langle\psi_1|\psi_7\rangle$, are slightly higher than the corresponding overlap in **1**-TS, $\langle\psi_1|\psi_7\rangle$ (see Tables 3 and 5 and Figure 8), but they are still far too low to suggest noteworthy bonding interactions. The sequence of overlaps between adjacent SC orbitals in **3**-TS and the shapes of these orbitals (see Figure 7) suggest that the SC wavefunction describes the combination of two largely independent fragments, an open-chain pentadienyl cation, with a π system described by orbitals ψ_1–ψ_5, and an ethene-like moiety, with a π system described by orbitals ψ_6 and ψ_7.

Place Figure 7, Table 5 and Figure 8 near here.

The pair of SC orbitals constrained to be orthogonal in the SC(6,7) calculation for **3** were ψ_2 and ψ_4. The data in Table 5 shows that, similarly to the situation with the analogous constraint used for **1**-TS, this restriction is very unlikely to have other than a negligible effect on the active space orbitals, as only a small overlap between non-adjacent SC orbitals is set equal to zero; the magnitude of the corresponding $\langle\psi_2|\psi_4\rangle$ overlap in **1** is rather low (0.101). Just as in **1** and **1**-TS, and in **2** and **2**-TS, none of the overlaps between non-adjacent SC orbitals in **3** and **3**-TS are large enough to suggest important bonding interactions.

A closer look at the composition of the spin space from the SC(6,7) wavefunction for **3** (see Figure 9, the Rumer diagrams included in this figure follow the conventions adopted in Figure 4) shows that it has certain features in common with the analogous spin space for **1** (see Figure 4), but there are necessarily also significant differences. Whereas the conjugated chain closed by the methylene bridge in **1** involves seven carbon atoms, the conjugated chain between the two methylene bridges in **3** is shorter, including only five carbon atoms. As a consequence, the two most important Kekulé-style Rumer spin functions in **1** can have no equivalents in **3**. Instead, the two most important Rumer spin functions in **3**, which are also Kekulé-style and couple to singlets the spins of three pairs of neighboring SC orbitals, create three bonds which involve two singlet pairs across the methylene bridges and a third singlet pair associated with an almost π bond. Just as in **1**, the two Rumer spin functions which are next in importance in **3**, $(1-2, 3-4, 5-6)$ and $(1-7, 2-3, 4-5)$, are also Kekulé-style and create a sequence of two almost π bonds that are followed by a bond across a methylene bridge. The two Kekulé-style Rumer spin functions with lowest weights in **3**, $(1-2, 3-4, 6-7)$ and $(2-3, 4-5, 6-7)$, demonstrate that, similarly to the situation observed in **1**, a bond across a methylene bridge is less capable of sustaining conjugation than is a carbon-carbon single bond; the bonding patterns associated with these Rumer spin functions resemble combinations of butadiene-like and ethene-like conjugated fragments. Just as in **1**, all

Place Figure 9 near here.

non-Kekulé-style Rumer spin functions in **3** with individual weights higher than 3% involve one "long diagonal" bond; two of the Rumer spin functions with one "long diagonal" bond, $(1-4, 2-3, 5-6)$ and $(1-7, 2-5, 3-4)$, turned out to have marginally higher weights than the two least important of the Kekulé-style Rumer spin functions. Taken together, the Rumer spin functions for **3** shown in Figure 9 account for a little under 85% of the spin space. This proportion is very close to the corresponding sum of over 84% for the Rumer spin functions for **1** shown in Figure 4, and suggests significant resonance. However, as the values of the overlap integrals between adjacent SC orbitals around the ring in **3** alternate much more than in **1** (*vide supra*), the SC description of **3** suggests that it is aromatic, but not to the level of **1**.

Our suggestion that the SC(6,7) wavefunction for **3**-TS appears to describe a combination of two largely independent fragments, an open-chain pentadienyl cation and an ethene-like moiety, was made after examining the overlaps between adjacent SC orbitals and the shapes of these orbitals (*vide supra*). This viewpoint is reinforced by the spin-coupling pattern for this system, shown in Figure 9. All five Rumer spin functions with weights over 3%, with a combined weight of *ca.* 89%, include a singlet pair over the ethene-like fragment and different modes of spin coupling over the pentadienyl cation fragment; of these, the most important one places the positive charge at position 3. Therefore, the analysis of the SC(6,7) wavefunction for **3**-TS identifies it as a non-aromatic system.

3 Conclusions

SC theory was used to obtain modern VB descriptions of the electronic structures of three cyclic systems which have been considered to involve homoconjugation and to exhibit homoaromaticity: the homotropenylium ion, $C_8H_9^+$, neutral cycloheptatriene, C_7H_8, and the 1,3-bishomotropenylium ion, $C_9H_{11}^+$. For each of these systems we studied both the C_s local minimum geometry and a C_{2v} TS geometry. The fully-variational SC wavefunctions for these systems, SC(6,7) for the homotropenylium and 1,3-bishomotropenylium ions and SC(6) for neutral cycloheptatriene, were found to recover a high proportion (between 94.4% and 97.9%) of the correlation energy included in the corresponding CASSCF(6,7) and CASSCF(6,6) wavefunctions. This confirms that these SC wavefunctions for the homotropenylium and 1,3-bishomotropenylium ions and for neutral cycloheptatriene can be viewed as easier-to-interpret, more compact alternatives to CASSCF wavefunctions that employ analogous active spaces.

The SC description of homoconjugation shows that the SC orbitals on both sides of an intervening methylene bridge change their shapes from the usual atom-centered $C(2p_\pi)$ orbitals with small protrusions towards neighboring orbitals, seen in many SC calculations on conjugated systems, to two-center orbitals with $C(2p_\pi)$ character spread unevenly between the carbon atoms on the two sides of the methylene bridge and with some C(2s) character. These orbitals overlap across a methylene bridge, providing a bonding interaction that has elements of both σ and π bonds. This bonding interaction does not develop if the distance between the carbon atoms on the two sides of the methylene bridge is sufficiently large, as in the local minimum geometry of neutral cycloheptatriene and in all three of the TS geometries. In such cases, the SC orbitals on both sides of a methylene bridge retain their atom-centred $C(2p_\pi)$ shapes and overlap very little. The SC results have also shown that the differences between "no-bond" and "bond" homoconjugated systems are much smaller than previously thought; the shapes of the SC orbitals on the two sides of a methylene bridge can evolve into typical sp^3 hybrids, engaged in a σ bond, upon a

sufficient decrease of the distance between the carbon atoms on either side of the bridge. On the other hand, increasing the distance between these carbon atoms leads to these two orbitals becoming more C($2p_\pi$)-like and interacting rather less with one another.

Analysis of the SC wavefunctions for the local minimum geometries of the homotropenylium and 1,3-bishomotropenylium ions shows that homoconjugation allows the establishment, in both species, of a cyclic arrangement of overlapping SC orbitals and of a resonance pattern that are rather similar to those for the tropylium cation.[18] The shapes of the SC orbitals, the values of the overlap integrals between adjacent SC orbitals and the compositions of the resonance patterns strongly suggest that both of the homotropenylium and 1,3-bishomotropenylium ions are aromatic, with the ordering 1,3-bishomotropenylium ion < homotropenylium ion < tropylium cation. The orbital interaction associated with the SC description of homoconjugation is essential for the emergence of this type of aromaticity, which can be rightly called homoaromaticity. For the cases in which we did not detect such homoconjugation, namely the local minimum geometry of neutral cycloheptatriene and all three TS geometries, the SC results suggest instead that each of these is non-aromatic.

Author Information

Corresponding Authors

*Peter B. Karadakov. E-mail: peter.karadakov@york.ac.uk. Telephone: +44 1904 322555.

*David L. Cooper. E-mail: dlc@liverpool.ac.uk. Telephone: +44 151 7943532.

Notes

The authors declare no competing financial interest.

References

(1) Cremer, D.; Childs, R. F.; Kraka, E. Cyclopropyl Homoconjugation, Homoaromaticity and Homoantiaromaticity: Theoretical Aspects and Analysis. In *The Chemistry of the Cyclopropyl Group*; Rappoport, Z., Ed.; J. Wiley and Sons: Chichester, 1995, Vol. 2, pp. 339–410.

(2) Chen, Z.; Jiao, H.; Wu, J. I.; Herges, R.; Zhang, S. B.; Schleyer, P. v. R. Homobenzene: Homoaromaticity and Homoantiaromaticity in Cycloheptatrienes. *J. Phys. Chem. A* **2008**, *112*, 10586–10594.

(3) Zhang, Q.; Yue, S.; Lu, X.; Chen, Z.; Huang, R.; Zheng, L.; Schleyer, P. v. R. Homoconjugation/Homoaromaticity in Main Group Inorganic Molecules. *J. Am. Chem. Soc.* **2009**, *131*, 9789–9799.

(4) Allan, C. S. M.; Rzepa, H. S. Chiral Aromaticities. A Topological Exploration of Möbius Homoaromaticity. *J. Chem. Theory Comput.* **2008**, *4*, 1841–1848.

(5) Bader, R. F. W. *Atoms in Molecules: A Quantum Theory*; Oxford University Press: Oxford, 1990.

(6) Savin, A.; Silvi, B.; Colonna, F. Topological Analysis of the Electron Localization Function Applied to Delocalized Bonds. *Can. J. Chem.* **1996**, *74*, 1088–1096.

(7) Cremer, D.; Kraka, E.; Slee, T. S.; Bader, R. F. W.; Lau, C. D. H.; Nguyen-Dang, T. T.; MacDougall, P. J. Description of Homoaromaticity in Terms of Electron Distributions. *J. Am. Chem. Soc.* **1983**, *105*, 5069–5075.

(8) Lepetit, C.; Silvi, B.; Chauvin, R. ELF Analysis of Out-of-Plane Aromaticity and In-Plane Homoaromaticity in Carbo[N]annulenes and [N]Pericyclynes. *J. Phys. Chem. A* **2003**, *107*, 464–473.

(9) Haddon, R. C. *J. Am. Chem. Soc.* A Perturbational Molecular Orbital (PMO) Theory of Homoaromaticity. **1975**, *97*, 3608–3615.

(10) Gerratt, J.; Lipscomb, W. N. Spin-Coupled Wave Functions for Atoms and Molecules. *Proc. Natl. Acad. Sci. (USA)* **1968**, *59*, 332–335.

(11) Karadakov, P. B.; Gerratt, J.; Cooper, D. L.; Raimondi, M. Core-Valence Separation in the Spin-Coupled Wave Function: A Fully Variational Treatment Based on a Second-Order Constrained Optimization Procedure. *J. Chem. Phys.* **1992**, *97*, 7637–7655.

(12) Ladner, R. C.; Goddard III, W. A. Improved Quantum Theory of Many-Electron Systems. V. The Spin-Coupling Optimized GI Method. *J. Chem. Phys.* **1969**, *51*, 1073–1087.

(13) Cooper, D. L.; Karadakov, P. B. Spin-Coupled Descriptions of Organic Reactivity. *Int. Rev. Phys. Chem.* **2009**, *28*, 169–206.

(14) Cooper, D. L.; Gerratt, J.; Raimondi, M. The Electronic Structure of the Benzene Molecule. *Nature* **1986**, *323*, 699–701.

(15) Gerratt, J. Modern Valence Bond Theory: Was Kekulé Right? *Chem. Br.* **1987**, *23*, 327–329.

(16) Cooper, D. L.; Wright, S. C.; Gerratt, J.; Hyams, P. A.; Raimondi, M. The Electronic Structure of Heteroaromatic Molecules. Part 3. A Comparison of Benzene, Borazine, and Boroxine. *J. Chem. Soc. Perkin Trans. II* **1989**, 719–724.

(17) Rumer, G. Zur Theorie der Spinvalenz. *Göttinger Nachr.* **1932**, *3*, 337–341.

(18) Karadakov, P. B.; Cooper, D. L.; Duke, B. J.; Li, J. Spin-Coupled Theory for 'N Electrons in M Orbitals' Active Spaces *J. Phys. Chem. A* **2012**, *116*, 7238–7244.

(19) Cremer, D.; Reichel, F.; Kraka, E. Homotropenylium Cation: Structure, Stability, and Magnetic Properties. *J. Am. Chem. Soc.* **1991**,*113*, 9459–9466.

(20) Frisch, M. J.; Trucks, G. W.; Schlegel, H. B.; Scuseria, G. E.; Robb, M. A.; Cheeseman, J. R.; Scalmani, G.; Barone, V.; Mennucci, B.; Petersson, G. A. et al. *Gaussian 09*, Revision D.01; Gaussian, Inc.: Wallingford, CT, 2013.

(21) Moran, D.; Simmonett, A. C.: Leach III, F. E.: Allen, W. D.; Schleyer, P. v. R.; Schaefer III, H. F. Popular Theoretical Methods Predict Benzene and Arenes to Be Nonplanar. *J. Am. Chem. Soc.* **2006**, *128*, 9342–9343.

(22) Karadakov, P. B. Do Large Polycyclic Aromatic Hydrocarbons and Graphene Bend? How Popular Theoretical Methods Complicate Finding the Answer to This Question. *Chem. Phys. Lett.* **2016**, *646*, 190–196.

(23) Fliegl, H.; Sundholm, D.; Taubert, S.; Jusélius, J.; Klopper, W. Magnetically Induced Current Densities in Aromatic, Antiaromatic, Homoaromatic, and Nonaromatic Hydrocarbons. *J. Phys. Chem. A*, **2009**, *113*, 8668–8676.

(24) Thorsteinsson, T.; Cooper, D. L.; Gerratt, J.; Karadakov, P. B.; Raimondi, M. Modern Valence Bond Representations of CASSCF Wavefunctions. *Theor. Chim. Acta*, **1996**, *93*, 343–366.

(25) Cooper, D. L.; Thorsteinsson, T.; Gerratt, J. Modern VB Representations of CASSCF Wave Functions and the Fully-Variational Optimization of Modern VB Wave Functions Using the CASVB Strategy. *Adv. Quant. Chem.* **1998**, *32*, 51–67.

(26) Thorsteinsson, T.; Cooper, D. L. Nonorthogonal Weights of Modern VB Wave functions. Implementation and Applications within CASVB. *J. Math. Chem.* **1998**, *23*, 105–126.

(27) Thorsteinsson, T.; Cooper, D. L. An Overview of the CASVB Approach to Modern Valence Bond Calculations. In *Quantum Systems in Chemistry and Physics. Volume 1: Basic Problems and Model Systems*; Hernández-Laguna, A.; Maruani, J.; McWeeny, R.; Wilson, S., Eds.; Kluwer: Dordrecht, 2000, pp. 303–326.

(28) Werner, H.-J.; Knowles, P. J.; Knizia, G.; Manby, F. R.; Schütz, M. Molpro: A General-Purpose Quantum Chemistry Program Package. *WIREs Comput. Mol. Sci.* **2012**, *2*, 242–253.

(29) Werner, H.-J.; Knowles, P. J.; Knizia, G.; Manby, F. R.; Schütz, M.; Celani, P.; Korona, T.; Lindh, R.; Mitrushenkov, A.; Rauhut, G. et al. *MOLPRO*, version 2012.1: Cardiff, U.K.

(30) Sironi, M.; Raimondi, M.; Cooper, D. L.; Gerratt, J. The Unusual Coordination of Carbon Atoms in Bicyclic 1,6-methano[10]annulene: A Modern Valence Bond Study. *J. Mol. Struct. Theochem* **1995**, *338*, 257–265.

(31) Chirgwin, B. H.; Coulson, C. A. The Electronic Structure of Conjugated Systems. VI. *Proc. Roy. Soc. Lond. Ser. A* **1950**, *201*, 196–209.

(32) Reindl, B.; Clark, T,; Schleyer, P. v. R. Modern Molecular Mechanics and Ab Initio Calculations on Benzylic and Cyclic Delocalized Cations. *J. Phys. Chem. A* **1998**, *102*, 8953–8963.

(33) Gibson, C. M.; Havenith, R. W. A.; Fowler, P. W.; Jenneskens, L. W. Planar Homotropenylium Cation: A Transition State with Reversed Aromaticity. *J. Org. Chem.* **2015**, *80*, 1395–1401.

(34) Fliegl, H.; Taubert, S.; Lehtonen, O.; Sundholm, D. The Gauge Including Magnetically Induced Current Method. *Phys. Chem. Chem. Phys.* **2011**, *13*, 20500–20518.

(35) Schaftenaar, G.; Noordik, J. H. Molden: A Pre- and Post-Processing Program for Molecular and Electronic Structures. *J. Comput.-Aided Mol. Des.* **2000**, *14*, 123–134.

Tables and Figures

Table 1: The four lowest vibrational frequencies of the C_s symmetry local minimum and C_{2v} symmetry TS geometries of the homotropenylium ion calculated at the MP2(Full)/cc-pVTZ and MP2(Full)/6-31G(d) levels of theory (in cm^{-1}, normal mode symmetries in brackets).

Geometry	Method	$\tilde{\nu}_1$	$\tilde{\nu}_2$	$\tilde{\nu}_3$	$\tilde{\nu}_4$
C_s local minimum	MP2(Full)/6-31G(d)	217.4 (a'')	226.5 (a')	309.8 (a')	333.7 (a'')
	MP2(Full)/cc-pVTZ	213.5 (a'')	225.2 (a')	307.7 (a')	326.2 (a'')
C_{2v} TS	MP2(Full)/6-31G(d)	166.3i (b_1)	100.2 (a_2)	233.7 (b_1)	309.3 (a_1)
	MP2(Full)/cc-pVTZ	135.3i (b_1)	112.6 (a_2)	264.5 (b_1)	303.2 (a_1)

Table 2: Total HF, SC and CASSCF energies (in E_h) of **1**, **1**-TS, **2**, **2**-TS, **3** and **3**-TS, percentages of recovered CASSCF correlation energy (in brackets), and numbers of CSFs included in the SC and CASSCF wavefunctions [cc-pVTZ basis, MP2(Full)/cc-pVTZ geometries].

Wavefunction	CSFs	System	Total Energy	System	Total Energy
HF	1	**1**	−307.981 558	**1**-TS	−307.958 867
SC(6,7)	35		−308.059 503 (94.9%)		−308.034 496 (95.4%)
CASSCF(6,7)	490		−308.063 717		−308.038 182
HF	1	**2**	−269.768 385	**2**-TS	−269.765 951
SC(6)	5		−269.843 822 (96.6%)		−269.845 507 (97.9%)
CASSCF(6,6)	175		−269.846 462		−269.847 202
HF	1	**3**	−346.971 648	**3**-TS	−347.038 182
SC(6,7)	35		−347.049 022 (94.4%)		−346.962 062 (97.1%)
CASSCF(6,7)	490		−347.053 597		−347.035 944

Table 3: Overlap integrals $\langle\psi_\mu|\psi_\nu\rangle$ between the SC orbitals from the SC(6,7) wavefunctions for **1** (top values) and for **1**-TS (bottom values).

	ψ_1	ψ_2	ψ_3	ψ_4	ψ_5	ψ_6	ψ_7
ψ_1	1.000	0.358 0.645	−0.184 −0.026	−0.191 −0.019	−0.222 0.042	−0.199 0.002	0.498 0.005
ψ_2		1.000	0.469 0.301	−0.102 −0.008	−0.149 0.002	−0.195 −0.031	−0.199 0.002
ψ_3			1.000	0.458 0.521	−0.066 0.000	−0.149 0.002	−0.222 0.042
ψ_4				1.000	0.458 0.521	−0.102 −0.008	−0.191 −0.019
ψ_5					1.000	0.469 0.301	−0.184 −0.026
ψ_6						1.000	0.358 0.645
ψ_7							1.000

Table 4: Overlap integrals $\langle\psi_\mu|\psi_\nu\rangle$ between the SC orbitals from the SC(6) wavefunctions for **2** (top values) and for **2**-TS (bottom values).

	ψ_1	ψ_2	ψ_3	ψ_4	ψ_5	ψ_6
ψ_1	1.000	0.647 0.653	0.069 0.086	−0.004 0.033	0.054 0.010	0.174 0.016
ψ_2		1.000	0.298 0.311	0.058 0.071	−0.047 −0.043	0.054 0.010
ψ_3			1.000	0.645 0.642	0.058 0.071	−0.004 0.033
ψ_4				1.000	0.298 0.311	0.069 0.086
ψ_5					1.000	0.647 0.653
ψ_6						1.000

Table 5: Overlap integrals $\langle\psi_\mu|\psi_\nu\rangle$ between the SC orbitals from the SC(6,7) wavefunctions for **3** (top values) and for **3**-TS (bottom values).

	ψ_1	ψ_2	ψ_3	ψ_4	ψ_5	ψ_6	ψ_7
ψ_1	1.000	0.290 0.582	0.135 −0.181	−0.100 −0.160	−0.216 −0.066	−0.222 0.013	0.587 0.066
ψ_2		1.000	0.506 0.378	0.000 −0.101	−0.100 −0.160	−0.143 −0.003	−0.191 0.002
ψ_3			1.000	0.506 0.378	−0.135 −0.181	−0.185 −0.024	−0.185 −0.024
ψ_4				1.000	0.290 0.582	−0.191 0.002	−0.143 −0.003
ψ_5					1.000	0.587 0.066	−0.222 0.013
ψ_6						1.000	0.176 0.662
ψ_7							1.000

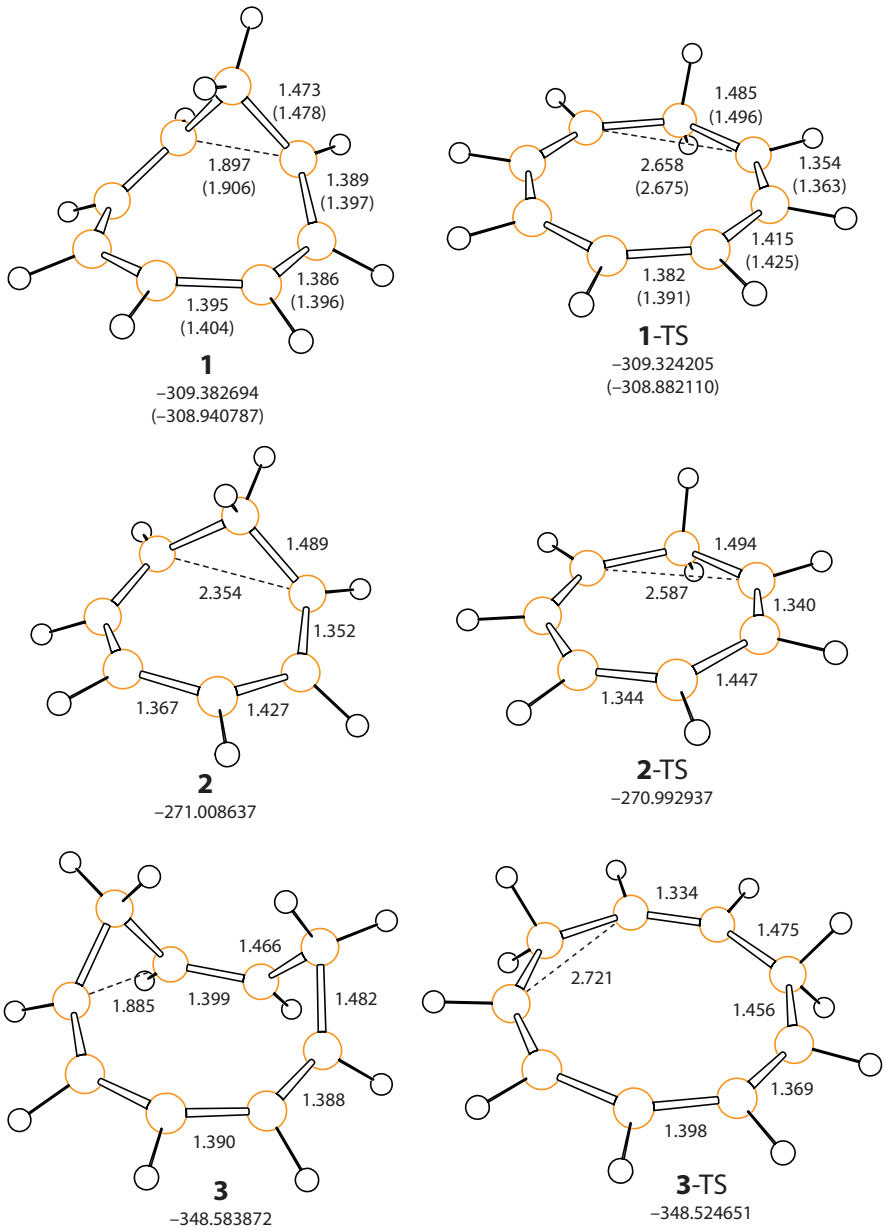

Figure 1: C_s symmetry local minimum and C_{2v} symmetry TS geometries of the homotropenylium ion (**1** and **1**-TS), neutral cycloheptatriene (**2** and **2**-TS), and the 1,3-bishomotropenylium ion (**3** and **3**-TS), optimized at the MP2(Full)/cc-pVTZ level of theory. Unique carbon-carbon bond lengths in Å, energies (under structures) in E_h. Numbers in brackets for **1** and **1**-TS correspond to MP2(Full)/6-31G(d) results.

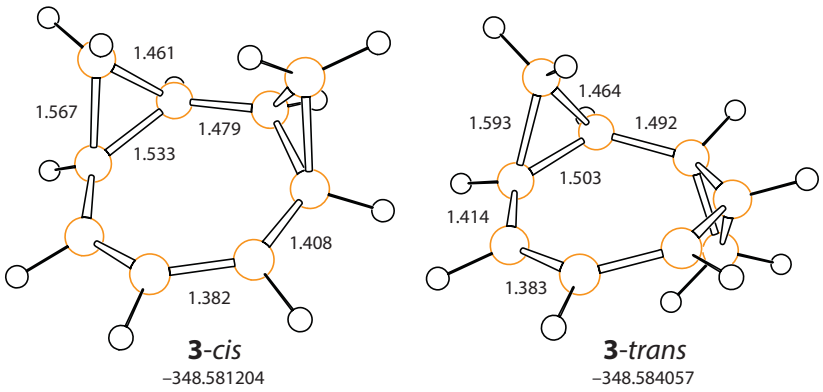

Figure 2: C_s (**3**-*cis*) and C_2 (**3**-*trans*) symmetry local minimum geometries of the 1,3-bishomotropenylium ion optimized at the MP2(Full)/cc-pVTZ level of theory. Unique carbon-carbon bond lengths in Å, energies (under structures) in E_h.

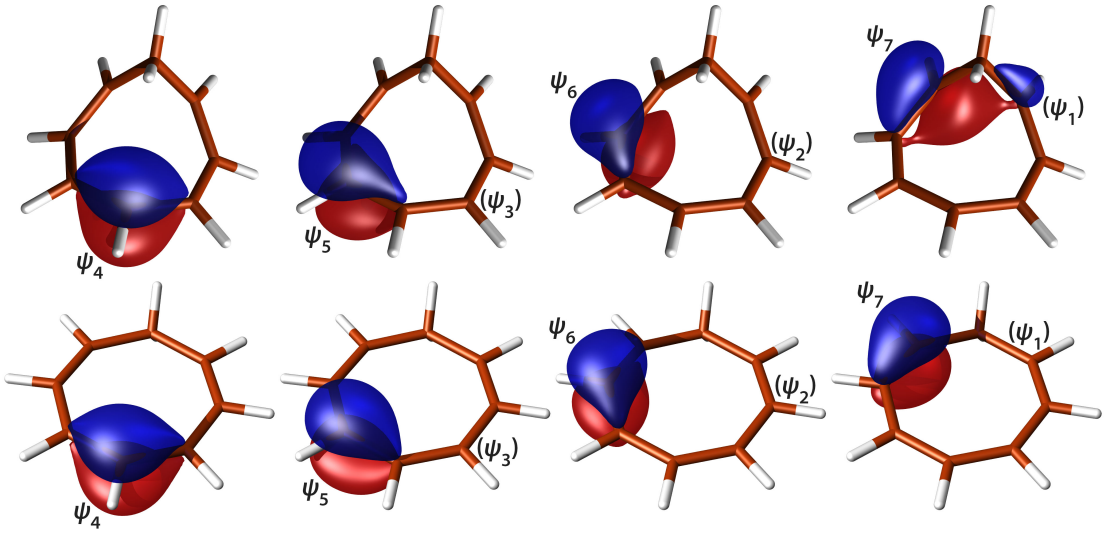

Figure 3: Symmetry-unique SC orbitals from the SC(6,7) wavefunctions for **1** (top row) and for **1**-TS (bottom row), as isovalue surfaces at $\psi_\mu = \pm 0.08$. Orbital symbols in brackets, (ψ_1)–(ψ_3), indicate the positions of the symmetry-related partners of orbitals ψ_5–ψ_7. POV-Ray (Persistence of Vision Ray-tracer) files for the isovalue surfaces were generated by MOLDEN.[35] For further details, see the text.

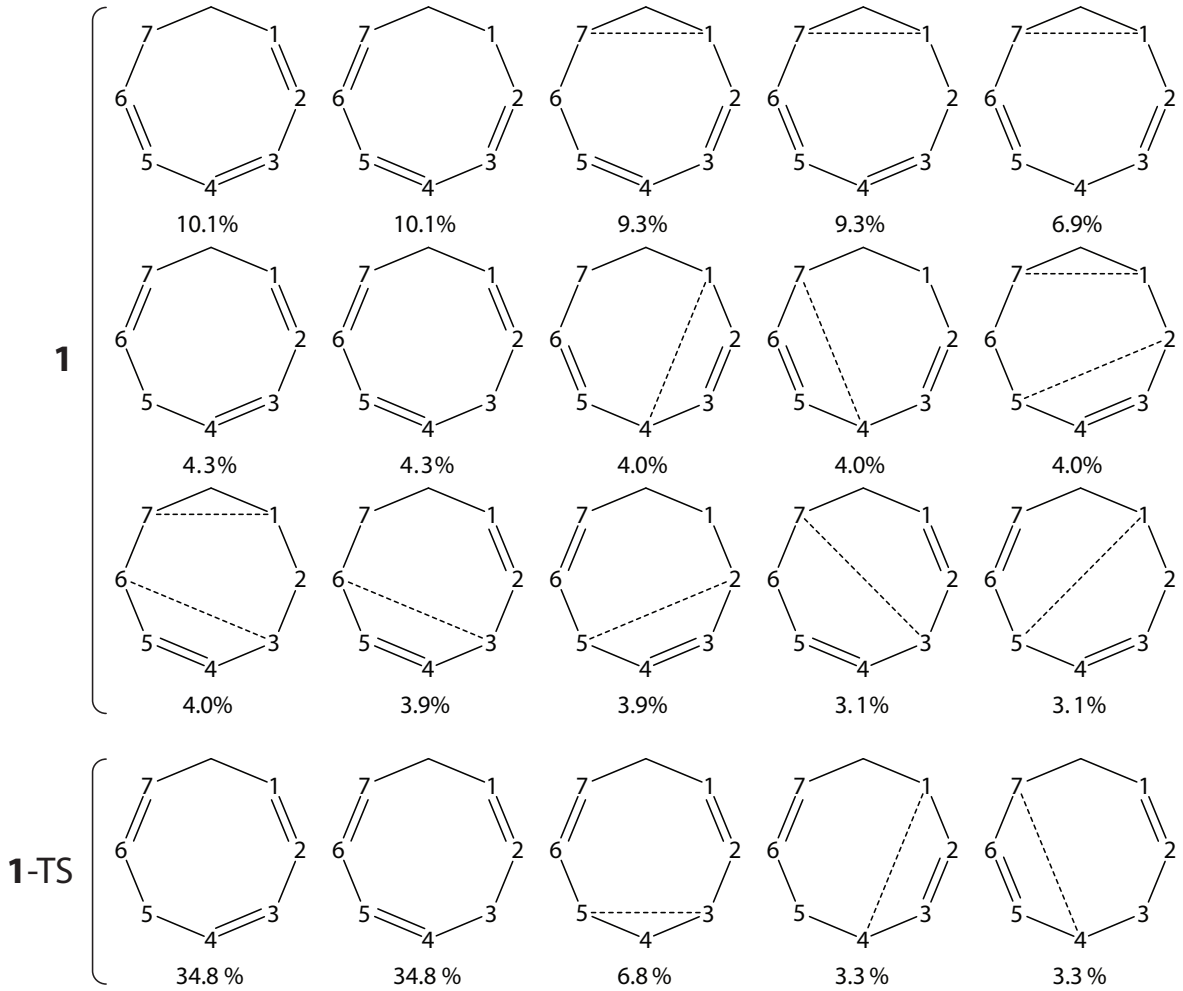

Figure 4: Rumer spin functions with individual Chirgwin-Coulson weights higher than 3% from the spin spaces associated with the SC(6,7) wavefunctions for **1** and for **1**-TS, in order of declining importance in each case.

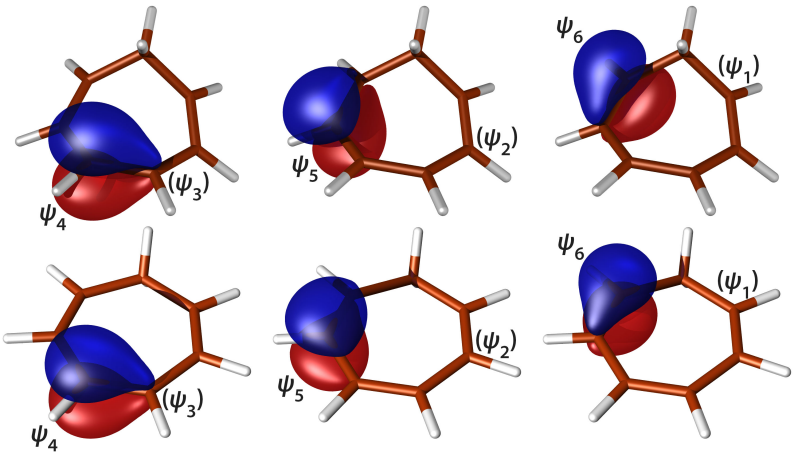

Figure 5: Symmetry-unique SC orbitals from the SC(6) wavefunctions for **2** (top row) and for **2**-TS (bottom row), as isovalue surfaces at $\psi_\mu = \pm 0.08$. Orbital symbols in brackets, (ψ_1)–(ψ_3), indicate the positions of the symmetry-related partners of orbitals ψ_4–ψ_6. For further details, see the caption to Figure 3 and also the text.

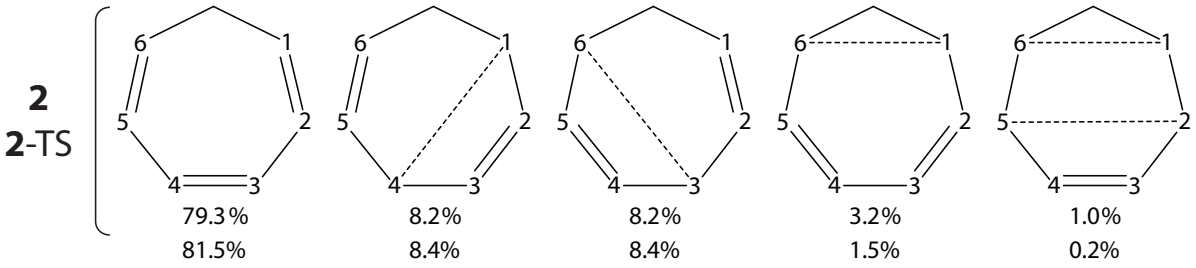

Figure 6: Chirgwin-Coulson weights of the Rumer spin functions from the spin spaces associated with the SC(6) wavefunctions for **2** (top values) and for **2**-TS (bottom values), in order of declining importance.

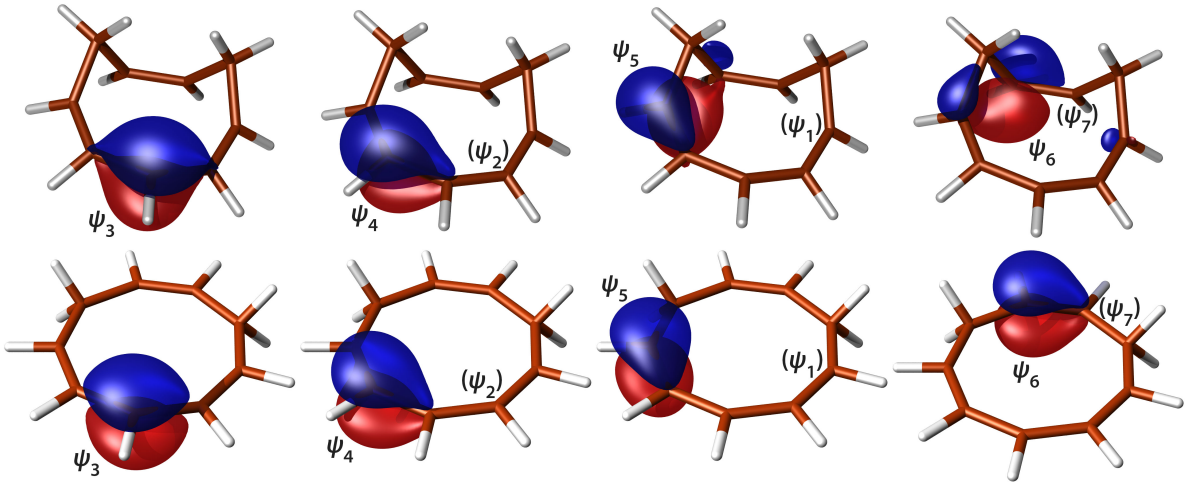

Figure 7: Symmetry-unique SC orbitals from the SC(6,7) wavefunctions for **3** (top row) and for **3**-TS (bottom row), as isovalue surfaces at $\psi_\mu = \pm 0.08$. Orbital symbols in brackets, (ψ_1), (ψ_2) and (ψ_7), indicate the positions of the symmetry-related partners of orbitals ψ_5, ψ_4 and ψ_6, respectively. For further details, see the caption to Figure 3 and also the text.

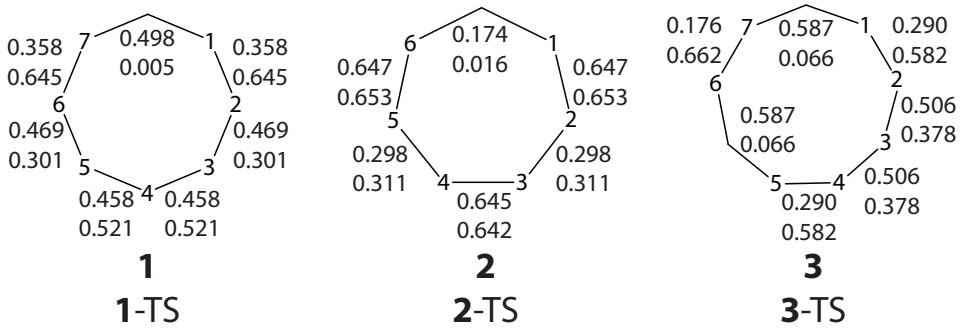

Figure 8: Overlap integrals between adjacent SC orbitals from the SC wavefunctions for **1**, **2** and **3** (top values), and for **1**-TS, **2**-TS and **3**-TS (bottom values). Overlap integrals between SC orbitals on the two sides of a methylene bridge are shown inside the rings.

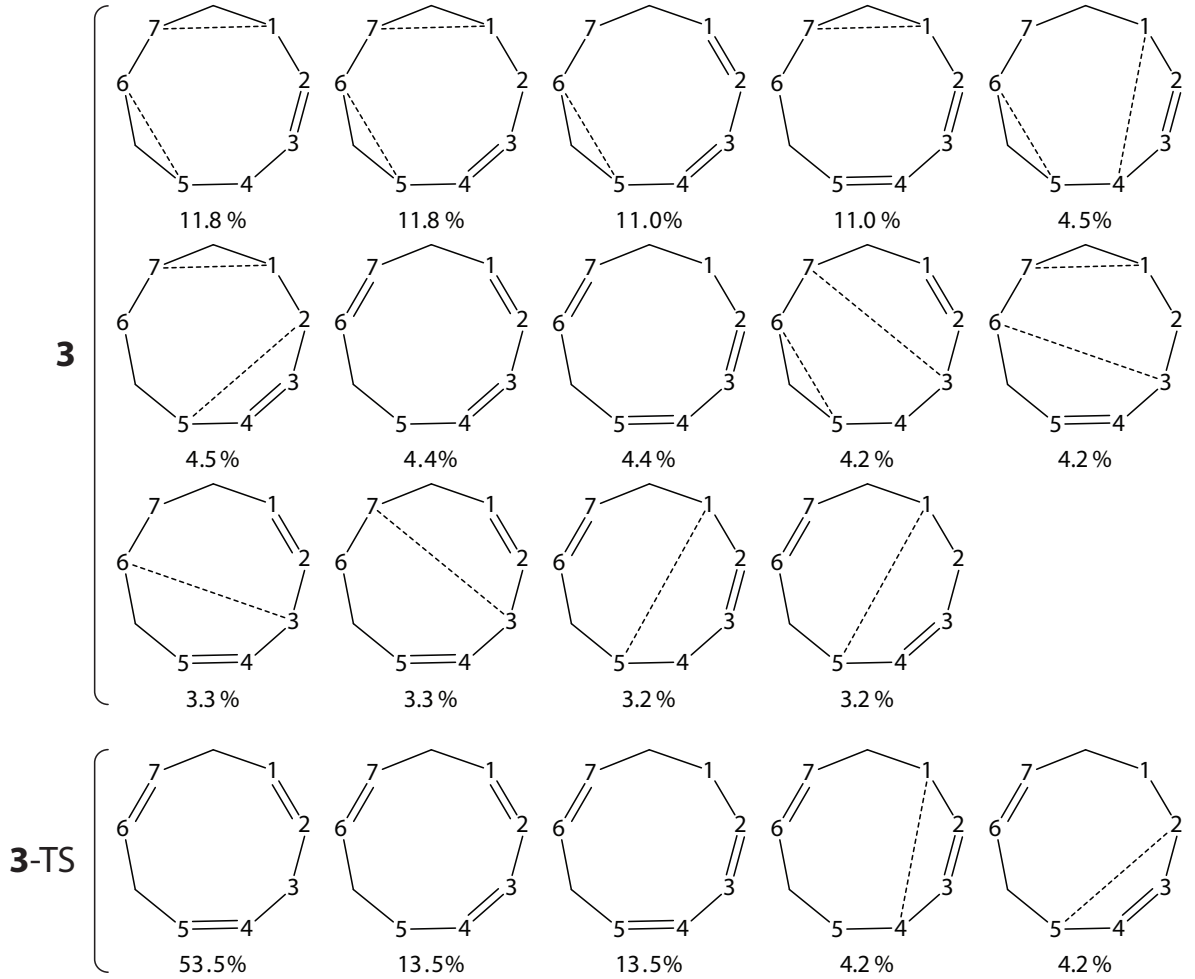

Figure 9: Rumer spin functions with individual Chirgwin-Coulson weights higher than 3% from the spin spaces associated with the SC(6,7) wavefunctions for **3** and for **3**-TS, in order of declining importance.

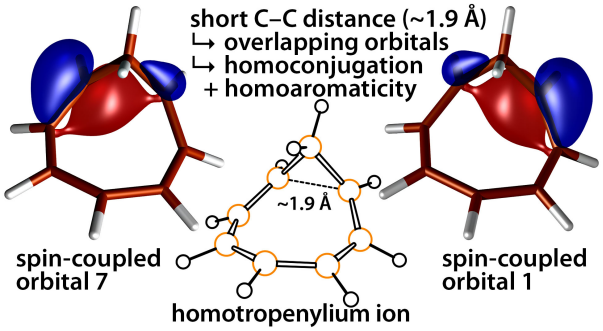
short C–C distance (~1.9 Å)
↳ overlapping orbitals
↳ homoconjugation
+ homoaromaticity
~1.9 Å
spin-coupled
orbital 7
spin-coupled
orbital 1
homotropenylium ion